Progress In Electromagnetics Research M, Vol. 27, 97–107, 2012

VECTOR MODE ANALYSIS OF OPTICAL WAVEGUIDES BY QUADRATIC SPLINE COLLOCATION METHOD

Jianwei Mu[1], Haibo Liang[2], Xun Li[2, *], Bin Xu[2], and Weiping Huang[2]

[1]Microphotonics Center and Department of Materials Science and Engineering, Massachusetts Institute of Technology, 77 Massachusetts Ave, Cambridge, MA 02139, USA

[2]Department of Electrical and Computer Engineering, McMaster University, 1280 Main Street West, Hamilton, Ontario L8S 4L8, Canada

Abstract—We present an accurate, efficient numerical analysis for vector modes of dielectric optical waveguide structures with an arbitrary refractive index profile using a quadratic spline collocation method (QSCM). The unknown weights of the polynomials are determined by forcing the errors at the collocation points to be zero. Consequently, the original second order differential equation is converted to a set of algebraic equations which can be solved by matrix techniques. The proposed QSCM method demonstrates better performance than the standard finite-difference method of the same convergence rate in terms of grid size with the same degree of computational complexity.

1. INTRODUCTION

Mode analysis for optical waveguides is usually the starting point for design and simulation of guided-wave photonic devices and integrated circuits. For most practical waveguide structures, analytical or even semi-analytical methods are rather limited in applicability [1]. In the past decades, researchers have proposed and developed various numerical methods; among which the finite-difference method (FDM) and the finite element method (FEM) are two of the most popular approaches [2–11]. The finite difference method (FDM) gains its popularity owing to its simplicity and effectiveness [4–11]. On the

Received 12 October 2012, Accepted 5 November 2012, Scheduled 15 November 2012

* Corresponding author: Xun Li (lixun@mcmaster.ca).

other hand, the finite element method (FEM) is more adaptive for complex waveguide structures with irregular interfaces [2, 3]. Some other methods which utilize global basis functions for representing the mode solutions have been reported in the literature though they are not as popular as FDM and FEM [12, 13].

As an optical mode solver, the ability to accurately simulate the vectorial properties of the optical field is critical in dealing with those strongly guided structures. This is of particular interest in silicon photonics due to the large index contrast in SOI (Silicon on Insulator) waveguides [14, 15].

Both FDM and FEM are built on localized unknown values, which naturally possess the flexibility to tackle the interfaces. With a small enough grid size, FDM and FEM will reach a certain required accuracy. On the opposite, due to their lacking of local treatment, those numerical mode solvers built on global bases or variables generally don't work for optical waveguides with high index contrast at interfaces or corners, unless the whole domain is divided into sub-domains, each of which will be approximated by its own whole-domain basis functions and interface conditions that are later imposed across adjacent sub-domains [16].

In this paper, we present a quadratic spline collocation method (QSCM), which uses a set of localized piecewise quadratic polynomials to approximate the exact mode solution. The unknown weights of the polynomials are then determined by forcing the errors at a set of points, called collocation points, to be zero. The original second order differential equation is therefore transferred to a set of algebraic equations, which can be solved by matrix techniques. Spline collocation method is considered as one of finite element methods (FEM) [17], as it utilizes finite element, namely, localized basis functions which can become infinitely small when the grid size of the computation window is decreased. However, the spline collocation method uses the weights of the basis-functions as the undetermined values and forces the approximation functions to exactly match the unknown functions at a set of points. Such approach is quite different from the traditional FEM, which chooses element nodes as the undetermined variables that can be solved by the variational principles or the Galerkin method [13].

Though the idea of collocation is not new in optics [18–22], the spline collocation based on the piecewise polynomials is rarely examined. Most of the available collocation approaches are based on orthogonal collocation [18–22], which use global basis functions that are nonzero throughout the whole computation domain. Such global collocation methods have difficulties in dealing with dielectric

interfaces where the field or the first-order derivative is discontinuous. Improvements on global collocation method have been reported when the computation domain is divided into sub-regions according to the position of the dielectric interfaces, and each sub-region is applied with global collocation, and finally, interface and boundary conditions are forced [16]. However, the increased complexity may impede its popularization.

The paper is structured as follow. We will brief the basic idea and the formulation of QSCM for boundary value problems, and will implement QSCM in the uniform region and dielectric interfaces in Section 2. In Section 3, various waveguide structures are evaluated with QSCM followed by comparison with the standard FDM result. We finally summarize our work in Section 4.

2. STRUCTURE AND WORKING PRINCIPLE

For a general two-point second-order boundary value problem, the computation domain (a, b) is divided into M uniform intervals with a grid size h, the middle points of which τ_i $(i = 1, 2, \ldots, M)$ are chosen as the collocation points. The quadratic basis functions are chosen as [17]

$$s_i(x) \equiv \frac{2}{3}\psi\left(\frac{x-a}{h} - i + 2\right) \quad i = 0, \ldots, M+1 \tag{1}$$

where

$$\psi(x) \equiv \begin{cases} 0 & x > 3 \text{ or } x < 0 \\ x^2 & 0 \le x \le 1 \\ -3 + 6x - 2x^2 & 1 \le x \le 2 \\ 9 - 6x + x^2 & 2 \le x \le 3 \end{cases} \tag{2}$$

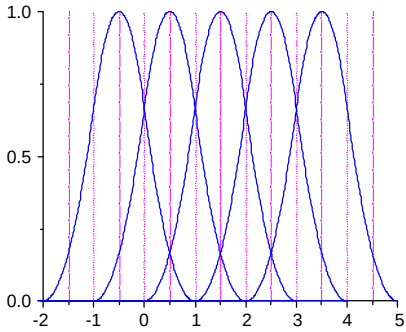

Figure 1. The quadratic spline collocation method basis functions example.

Figure 1 shows an example set of quadratic basis functions with computation domain (0, 3) and grid size 1.0. The collocation points are 0.5, 1.5, and 2.5. The boundary points are 0 and 3. Each of the piecewise quadratic basis functions have nonzero values only across three intervals as shown in Figure 1. This localization feature gives QSC flexibility for easy implementation for various boundary condition and discontinuity as discussed later.

The summation of the weighted basis functions [17]

$$\phi(x) = \sum_{i=0}^{M+1} \theta_i s_i(x) \quad i = 0, \ldots, M+1, \tag{3}$$

is formed as the approximate solution with unknown weights θ_j, which are determined by substituting Eq. (3) into the second order partial differential equation and the boundary conditions. For a longitudinally invariant waveguide, the full vector governing equations in magnetic field are given by

$$n^2 \frac{\partial}{\partial x}\left(\frac{1}{n^2}\frac{\partial H_y}{\partial x}\right) + \frac{\partial^2 H_y}{\partial y^2} + n^2 k^2 H_y - n^2 \frac{\partial}{\partial x}\left(\frac{1}{n^2}\frac{\partial H_x}{\partial y}\right) + \frac{\partial^2 H_x}{\partial x \partial y} = \beta^2 H_y \tag{4}$$

$$n^2 \frac{\partial}{\partial y}\left(\frac{1}{n^2}\frac{\partial H_x}{\partial y}\right) + \frac{\partial^2 H_x}{\partial x^2} + n^2 k^2 H_x - n^2 \frac{\partial}{\partial y}\left(\frac{1}{n^2}\frac{\partial H_y}{\partial x}\right) + \frac{\partial^2 H_y}{\partial x \partial y} = \beta^2 H_x \tag{5}$$

The boundary conditions used in this work are given by: for the discontinuity along y direction, H_x, H_y, $d(H_y)/d_y$, $d(H_y)/d_x$ are continuous; for the discontinuity along x direction, H_y, H_x, $d(H_x)/d_x$, $d(H_x)/d_y$ are continuous. It is worthy of noting that higher order boundary conditions will improve the accuracy. However, in this letter, we were trying to start with the simple boundary conditions to show the feasibility of the QSCM in mode solvers, the improved version incorporated with the higher order boundary conditions and the related applications such as beam propagation method are in development and will be presented in future publications. Substituting Eq. (3) into the Eq. (4) and Eq. (5), we have

$$Y_1 \bar{\theta}^{H_y} + X_1 \bar{\theta}^{H_x} = B_1 \bar{\theta}^{H_y} \tag{6}$$

$$Y_2 \bar{\theta}^{H_y} + X_2 \bar{\theta}^{H_x} = B_2 \bar{\theta}^{H_X} \tag{7}$$

here

$$\begin{aligned}
Y_1 &= D_2^{x'} \otimes D_0^y + D_0^x \otimes D_2^y + k_0^2 N D_0^x \otimes D_0^y \\
B_1 &= \beta^2 D_0^x \otimes D_0^y \\
X_2 &= D_2^x \otimes D_0^y + D_0^x \otimes D_2^{y'} + k_0^2 N D_0^x \otimes D_0^y \\
Y_2 &= -D_1^{x'} \otimes D_1^y + D_1^x \otimes D_1^y \\
Y_2 &= -D_1^{x'} \otimes D_1^y + D_1^x \otimes D_1^y
\end{aligned}$$

Here N is the distribution matrix for the permittivity (n^2), and the coefficient matrix for the zero-order, the first-order, and the second-order derivatives are given by [17]:

$$D_2^{x,y} = \frac{4}{3h_{x,y}^2}\begin{pmatrix} -3 & 1 & & & & & & \\ 1 & -2 & 1 & & & & & \\ & & & \cdots & & & & \\ & & & & 1 & -2 & 1 & \\ & & & & & 1 & -3 & \end{pmatrix} \tag{8}$$

$$D_1^{x,y} = \frac{2}{3h_{x,y}}\begin{pmatrix} 1 & 1 & & & & & & \\ -1 & 0 & 1 & & & & & \\ & & & \cdots & & & & \\ & & & & -1 & 0 & 1 & \\ & & & & & -1 & -1 & \end{pmatrix} \tag{9}$$

$$D_0^{x,y} = \frac{1}{6}\begin{pmatrix} 5 & 1 & & & & & & \\ 1 & 6 & 1 & & & & & \\ & & & \cdots & & & & \\ & & & & 1 & 6 & 1 & \\ & & & & & 1 & 5 & \end{pmatrix} \tag{10}$$

$D_0^{y'}$, $D_1^{y'}$, $D_2^{y'}$ are the modified coefficient matrices for the zero-order, the first-order and second-order derivative operators, respectively. Those modified coefficient matrices are obtained by modifying the basis function and imposing the boundary conditions. Assuming there are discontinuities at jth and $(j+1)$th points along y direction, the elements have to be modified as

$$D_0^{y'}(j,j) = \frac{1}{6}\left(\frac{n_{j+1}^2 - n_j^2}{n_{j+1}^2 + n_j^2} + 6\right) D_0^y(j,j)$$

$$D_0^{y'}(j,j+1) = \frac{2n_j^2}{n_{j+1}^2 + n_j^2} D_0^y(j,j+1)$$

$$D_0^{y'}(j+1,j) = \frac{2n_{j+1}^2}{n_{j+1}^2 + n_j^2} D_0^y(j+1,j)$$

$$D_0^{y'}(j+1,j+1) = \frac{1}{6}\left(\frac{n_j^2 - n_{j+1}^2}{n_{j+1}^2 + n_j^2} + 6\right) D_0^y(j+1,j+1)$$

for the zero-order derivative operators, and

$$D_1^{y'}(j,j) = \frac{n_{j+1}^2 - n_j^2}{n_{j+1}^2 + n_j^2} + D_1^y(j,j)$$

$$D_1^{y'}(j,j+1) = \frac{2n_j^2}{n_{j+1}^2 + n_j^2} D_1^y(j,j+1)$$

$$D_1^{y'}(j+1,j) = \frac{2n_{j+1}^2}{n_{j+1}^2+n_j^2} D_1^y(j+1,j)$$
$$D_1^{y'}(j+1,j+1) = -\frac{n_j^2-n_{j+1}^2}{n_{j+1}^2+n_j^2} + D_1^y(j+1,j+1)$$

for the first-order derivative operators, and

$$D_2^{y'}(j,j) = \frac{1}{2}\left(2-\frac{n_{j+1}^2-n_j^2}{n_{j+1}^2+n_j^2}\right) D_2^y(j,j)$$
$$D_2^{y'}(j,j+1) = \frac{2n_j^2}{n_{j+1}^2+n_j^2} D_2^y(j,j+1)$$
$$D_2^{y'}(j+1,j) = \frac{2n_{j+1}^2}{n_{j+1}^2+n_j^2} D_2^y(j+1,j)$$
$$D_2^{y'}(j+1,j+1) = \frac{1}{2}\left(2-\frac{n_j^2-n_{j+1}^2}{n_{j+1}^2+n_j^2}\right) D_2^y(j+1,j+1)$$

for the second-order derivative operators. Similarly, with the exchange of j to i and y to x, we can obtain the modified coefficient matrices $D_0^{x'}$, $D_1^{x'}$, $D_2^{x'}$, assuming there are discontinuities between ith and $(i+1)$th points along x direction. Finally we have $A\bar{\theta} = \beta^2 B\bar{\theta}$, which is a standard eigen-value problem in which the matrices are defined as

$$A = \begin{pmatrix} Y_1 & X_1 \\ Y_2 & X_2 \end{pmatrix}, \quad B = \begin{pmatrix} B_1 & 0 \\ 0 & B_2 \end{pmatrix} \tag{11}$$

For a two-dimensional waveguide structure, e.g., slab waveguide structures, Eqs. (4) and (5) become decoupled for the TM and TE modes, respectively.

$$n^2 \frac{\partial}{\partial x}\left(\frac{1}{n^2}\frac{\partial H_y}{\partial x}\right) + n^2 k^2 H_y = \beta_{TM}^2 H_y \tag{12a}$$
$$\frac{\partial^2 H_x}{\partial x^2} + n^2 k^2 H_x = \beta_{TE}^2 H_x \tag{12b}$$

In matrix form, we have

$$Y_{TM}\bar{\theta}^{H_y} = B_{TM}\bar{\theta}^{H_y} \tag{13a}$$
$$X_{TE}\bar{\theta}^{H_x} = B_{TE}\bar{\theta}^{H_X} \tag{13b}$$

Here

$$Y_{TM} = D_2^{x'} + k_0^2 N D_0^x$$
$$B_{TM} = \beta_{TM}^2 D_0^x$$
$$X_{TE} = D_2^{y'} + k_0^2 N D_0^y$$

$$B_{TE} = \beta_{TE}^2 D_0^y$$

It should be noted that, unlike in the FDM scheme where the (unknown) function is determined at a series of discrete points, the (unknown) function in the QSCM scheme is not only determined at a set of discrete points (i.e., the collocation points), but is also smoothed out by the local quadratic functions among the collocation points. Therefore, in a homogenous region where no abrupt change can possibly happen to the (unknown) function, the QSCM should be more accurate comparing to the FDM with a same set of discrete points. At the boundary of two different homogenous materials, however, the (unknown) function can have an abrupt change that cannot be described by a finite set of smooth functions. To solve this problem, we've modified the basis functions to explicitly represent the possible discontinuity in the (unknown) function. Such induced extra degree of freedom is then utilized to force the (unknown) function to satisfy the boundary condition embedded in the Maxwell equations. Hence the accuracy of the (unknown) function is ensured, not only inside the homogenous region, but also at the boundaries.

3. VERIFICATION OF QSC METHOD

To evaluate the QSCM mode solver performance, we compare it directly with a standard $O(h^2)$ finite difference (FD) mode solver. For a same grid size, a three-point scheme FD mode solver will result in the same tri-diagonal matrix as QSC. So the computation effort is roughly the same. The first structure we investigate is a three-layer asymmetric slab waveguide with a refractive index profile ($n_{clad} = 1.0$, $n_{core} = 3.5$, $n_{substrate} = 1.5$). The waveguide width is 0.6 μm, and the wavelength is

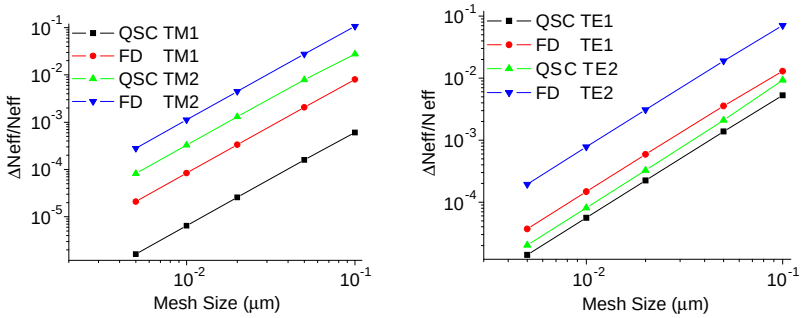

Figure 2. QSC and FD comparison with same grid size and computation effort.

1.55 μm. The slab waveguide structure is a good benchmark since it has analytical solutions. For the structure mentioned above, it supports three guided TE modes (Neff: 3.3457572/2.8514373/1.8943529) and two guided TM modes (Neff: 3.2707248/2.493801). The computation window is set to 5 micron meters and terminated with zero boundary condition. The results of the first two guided modes from FDM and QSC are shown in Figure 2 and it is observed that QSC has a better convergence rate.

Next we investigate two three-dimensional waveguides by calculating the normalized propagation constant and comparing results with those obtained by the finite difference method. For the rib waveguide in Figure 3(a), the thickness of the guiding layer d is 0.2 μm, and the height of the cladding h is 1.0 μm, the ridge width W is 2.4 μm. The other parameters have been shown in Figure 3. For purpose of comparison with the published results, we use the normalized propagation constant $B = (N_{eff}^2 - n_s^2)/(n_g^2 - n_s^2)$ for rib waveguide and the effective propagation constant for the channel waveguide.

The comparison of the current method with the published finite difference methods is shown in Figure 4. We also plot the field patterns of both rib and channel waveguide structures in Figure 5. With the decrease of the mesh size, both QSCM and FDM show the increased computation accuracy (Figure 4(a)). Since the decrease of the mesh size is equivalent to the increase of the number of the mesh points, it is reasonable that we see a convergence of the effective index with the increase of the mesh points (Figure 4(b)). Moreover, it is observed that QSCM and FDM mode solver have the same convergence rate. However, with the same grid size, namely the same amount of computation effort, QSCM mode solver is more accurate than conventional FDM mode solver [4, 5], however, it should be addressed that the current QSCM loses the advantage comparing to

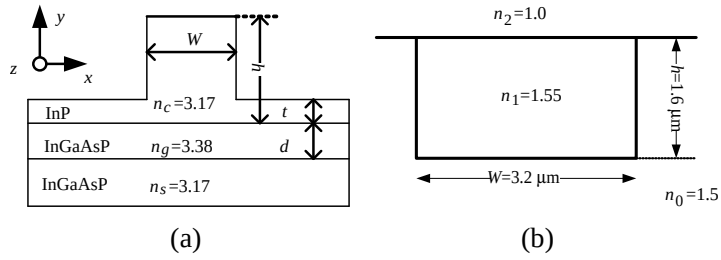

Figure 3. waveguide structures. (a) Rib waveguide [5]. (b) Channel waveguide [7].

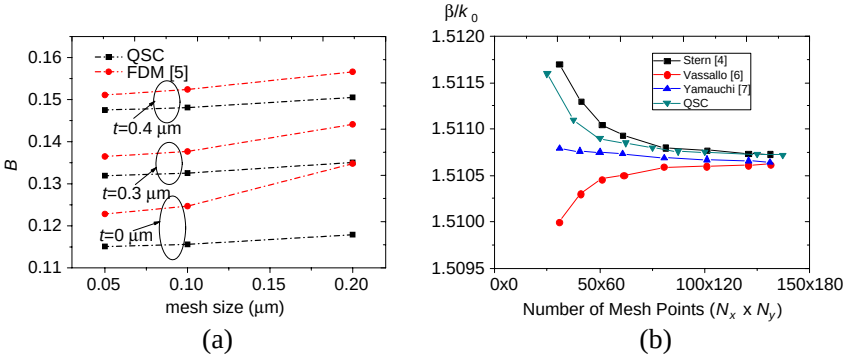

Figure 4. Comparison of QSC with finite difference method. (a) Rib waveguide. (b) Channel waveguide.

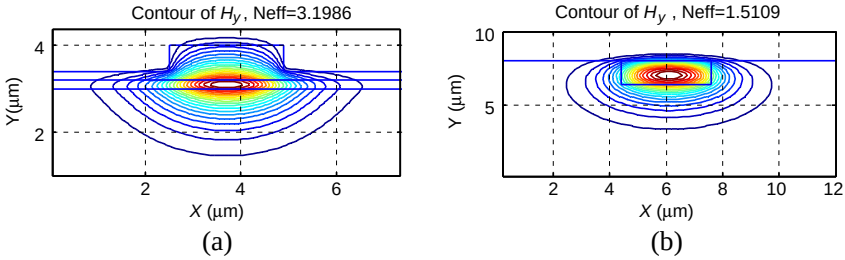

Figure 5. Field patterns calculated by QSC. (a) Rib waveguide ($t = 0.2$). (b) Channel waveguide.

the improved finite difference method [7, 10, 11] where higher order boundary conditions are applied. The improved QSCM with higher order boundary conditions will be our future work.

4. CONCLUSIONS

We have introduced a numerical mode solver based on the quadratic spline collocation method which employs piecewise second-order polynomials. The piecewise property of spline collocation method allows us to easily integrate the discontinuity of the dielectric interfaces into our formulation. The resulted QSCM mode solver performs well when it is compared with the standard finite difference method. This general method may find its applications of studying the optical characteristics of the photonic devices and applications in various eigen-modes associated methods such as beam propagation method, coupled mode theory, and mode expansion methods, etc.

REFERENCES

1. Huang, W. (ed.), *Methods for Modeling and Simulation of Guided-wave Optoelectronic Devices: Part I. Modes and Couplings,* EMW Publishing, Cambridge, MA, 1995.
2. Rahman, B. M. A. and J. B. Davies, "Finite-element analysis of optical and microwave waveguide problems," *IEEE Trans. Microwave Theory Tech.*, Vol. 32, No. 1, 20–28, 1984.
3. Koshiba, M. and K. Inoue, "Simple and efficient finite-element analysis of microwave and optical waveguides," *IEEE Trans. Microwave Theory Tech.*, Vol. 40, No. 2, 371–377, 1992.
4. Stern, M. S., "Semivectorial polarized finite difference method for optical waveguides with arbitrary index profiles," *IEE Proc. J.*, Vol. 135, No. 2, 56–63, 1988.
5. Xu, C. L., W. P. Huang, M. S. Stern, and S. K. Chaudhuri, "Full-vectorial mode calculations by finite difference method," *IEE Proc. Optoelectron.*, Vol. 142, No. 5, 281–286, 1994.
6. Vassallo, C., "Improvement of finite difference method for step-index optical waveguides," *Inst. Elect. Eng. Proc. — J.*, Vol. 139, No. 2, 137–142, 1992.
7. Yamauchi, J., M. Sekiguchi, O. Uchiyama, J. Shibayama, and H. Nakano, "Modified finite-difference formula for the analysis of semivectorial modes in step-index optical waveguides," *IEEE Photon. Technol. Lett.*, Vol. 9, 961–963, 1997.
8. Vassallo, C., "Interest of improved three-point formulas for finite-difference modeling of optical devices," *J. Opt. Soc. Amer.*, Vol. 14, 3273–3284, 1997.
9. Chiou, Y.-P., Y. C. Chiang, and H. C. Chang, "Improved three point formulas considering the interface conditions in the finite-difference analysis of step-index optical devices," *J. Lightwave Technology*, Vol. 18, No. 2, 243–251, 2000.
10. Chiou, Y.-P. and C.-H. Du, "Arbitrary-order full-vectorial interface conditions and higher-order finite-difference analysis of optical waveguides," *J. Lightwave Technology*, Vol. 29, No. 22, 3445–3452, Nov. 2011.
11. Chiou, Y.-P. and C.-H. Du, "Arbitrary-order interface conditions for slab structures and their applications in waveguide analysis," *OSA Optics Express*, Vol. 18, No. 5, 4088–4102, Mar. 2010.
12. Rogge, U. and R. Pregla, "Method of lines for the analysis of dielectric waveguides," *J. Lightwave Technology*, Vol. 11, 2015–2020, Dec. 1993.

13. Vassallo, C., "1993–1995 optical mode solvers," *Opt. Quantum Electron.*, Vol. 29, 95–114, 1997.
14. Celler, G. K. and S. Cristoloveanu, "Frontiers of silicon-on-insulator," *Applied Phys. Reviews*, Vol. 93, No. 9, 4955–4978, 2003.
15. Bogaerts, W., R. Baets, P. Dumon, et al., "Nanophotonic waveguides in silicon-on-insulator fabricated with CMOS technology," *J. Lightwave Technology*, Vol. 23, No. 1, 2005.
16. Chiang, P. J., C. L. Wu, et al., "Full-vectorial optical waveguide mode solvers using multidomain pseudospectral frequency-domain (PSFD) formulations," *IEEE J. Quantum Electronics*, Vol. 44, No. 1, 56–66, 2008.
17. Christara, C. C., "Quadratic spline collocation methods for elliptic partial differential equations," *BIT*, Vol. 34, No. 1, 33–61, 1994.
18. Sharma, A. and S. Banerjee, "Method for propagation of total fields or beams through optical waveguides," *Opt. Lett.*, Vol. 14, No. 1, 96–98, 1989.
19. Xiao, J. B. and X. H. Sun, "Full-vectorial mode solver for anisotropic optical waveguides using multidomain spectral collocation method," *Opt. Comm.*, Vol. 28, No. 14, 2835–2840, 2010.
20. Huang, C. X., C. C. Huang, and J. Y. Yang, "A full-vectorialpseudospectral modal analysis of dielectric optical waveguides with stepped refractive index profiles," *IEEE J. Sel. Top. Quantum Electron.*, Vol. 11, No. 2, 457–465, 2005.
21. Huang, C. C. and C. C. Huang, "An efficient and accurate semivectorial spectral collocation method for analyzing polarized modes of rib waveguides," *J. Lightwave Technology*, Vol. 23, No. 7, 2309–2317, 2005.
22. Chen, J. and Q. H. Liu, "A non-spurious vector spectral element method for Maxwell's equations," *Progress In Electromagnetics Research*, Vol. 96, 205–215, 2009.

HFSS视频培训课程推荐

HFSS 软件是当前最流行的微波无源器件和天线设计软件，易迪拓培训(www.edatop.com)是国内最专业的微波、射频和天线设计培训机构。

为帮助工程师能够更好、更快地学习掌握 HFSS 的设计应用，易迪拓培训特邀李明洋老师主讲了多套 HFSS 视频培训课程。李明洋老师具有丰富的工程设计经验，曾编著出版了《HFSS 电磁仿真设计应用详解》、《HFSS 天线设计》等多本 HFSS 专业图书。视频课程，专家讲解，直观易学，是您学习 HFSS 的最佳选择。

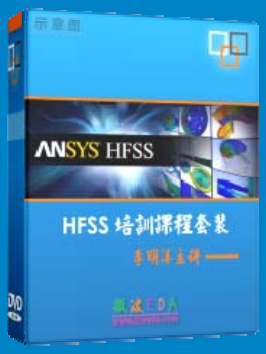

HFSS 学习培训课程套装

该套课程套装包含了本站全部 HFSS 培训课程，是迄今国内最全面、最专业的 HFSS 培训教程套装，可以帮助您从零开始，全面深入学习 HFSS 的各项功能和在多个方面的工程应用。购买套装，更可超值赠送 3 个月免费学习答疑，随时解答您学习过程中遇到的棘手问题，让您的 HFSS 学习更加轻松顺畅…

课程网址：http://www.edatop.com/peixun/hfss/11.html

HFSS 天线设计培训课程套装

套装包含 6 门视频课程和 1 本图书，课程从基础讲起，内容由浅入深，理论介绍和实际操作讲解相结合，全面系统的讲解了 HFSS 天线设计的全过程。是国内最全面、最专业的 HFSS 天线设计课程，可以帮助您快速学习掌握如何使用 HFSS 设计天线，让天线设计不再难…

课程网址：http://www.edatop.com/peixun/hfss/122.html

更多 HFSS 视频培训课程：

- **两周学会 HFSS —— 中文视频培训课程**
  课程从零讲起，通过两周的课程学习，可以帮助您快速入门、自学掌握 HFSS，是 HFSS 初学者的最好课程，网址：http://www.edatop.com/peixun/hfss/1.html
- **HFSS 微波器件仿真设计实例 —— 中文视频教程**
  HFSS 进阶培训课程，通过十个 HFSS 仿真设计实例，带您更深入学习 HFSS 的实际应用，掌握 HFSS 高级设置和应用技巧，网址：http://www.edatop.com/peixun/hfss/3.html
- **HFSS 天线设计入门 —— 中文视频教程**
  HFSS 是天线设计的王者，该教程全面解析了天线的基础知识、HFSS 天线设计流程和详细操作设置，让 HFSS 天线设计不再难，网址：http://www.edatop.com/peixun/hfss/4.html
- **更多 HFSS 培训课程**，敬请浏览：http://www.edatop.com/peixun/hfss

关于易迪拓培训：

易迪拓培训(www.edatop.com)由数名来自于研发第一线的资深工程师发起成立，一直致力和专注于微波、射频、天线设计研发人才的培养；后于 2006 年整合合并微波 EDA 网(www.mweda.com)，现已发展成为国内最大的微波射频和天线设计人才培养基地，成功推出多套微波射频以及天线设计相关培训课程和 ADS、HFSS 等专业软件使用培训课程，广受客户好评；并先后与人民邮电出版社、电子工业出版社合作出版了多本专业图书，帮助数万名工程师提升了专业技术能力。客户遍布中兴通讯、研通高频、埃威航电、国人通信等多家国内知名公司，以及台湾工业技术研究院、永业科技、全一电子等多家台湾地区企业。

我们的课程优势：

※ 成立于 2004 年，10 多年丰富的行业经验

※ 一直专注于微波射频和天线设计工程师的培养，更了解该行业对人才的要求

※ 视频课程、既能达到现场培训的效果，又能免除您舟车劳顿的辛苦，学习工作两不误

※ 经验丰富的一线资深工程师讲授，结合实际工程案例，直观、实用、易学

联系我们：

※ 易迪拓培训官网：http://www.edatop.com

※ 微波 EDA 网：http://www.mweda.com

※ 官方淘宝店：http://shop36920890.taobao.com